Int J Adv Manuf Technol (2012) 63:573–581
DOI 10.1007/s00170-012-3944-3

ORIGINAL ARTICLE

Prevention of humping bead associated with high welding speed by double-electrode gas metal arc welding

C. S. Wu · Z. H. Hu · L. M. Zhong

Received: 20 June 2011 / Accepted: 10 January 2012 / Published online: 31 January 2012

Abstract Manufacturing productivity can be improved by increasing the welding speed. However, humping bead will occur when welding speed is beyond a certain value. An experimental system of double-electrode gas metal arc welding (DE-GMAW) was developed to implement high speed welding and prevent from humping bead formation. The DE-GMAW appropriately partition the heat energy between the wire and the base metal so that higher deposition rate of filler wire and suitable shape and size of weld pool are ensured. The arc images captured during DE-GMAW process were used to optimize the geometric parameters between the gas tungsten arc welding and the gas metal arc welding (GMAW) torches. The main arc and bypass arc integrated well and satisfactory weld bead formation was obtained. Through observing the weld pool behaviors from side view during DE-GMAW process, it was found that the height of both solidified and molten region at the pool tail is almost flat so that no humping bead was formed during DE-GMAW with the welding speed up to 1.7 m/min. The side view images of weld pool in DE-GMAW were compared with those in conventional GMAW, and the reason why DE-GMAW can suppress humping bead is shortly discussed.

Keywords Preventing hump bead · High speed welding · Double-electrode gas metal arc welding

C. S. Wu (✉) · Z. H. Hu · L. M. Zhong
MOE Key Lab for Liquid–Solid Structure Evolution and Materials Processing, and Institute of Materials Joining,
Shandong University,
Jinan 250061, China
e-mail: wucs@sdu.edu.cn

C. S. Wu
State Key Lab of Advanced Welding & Joining,
Harbin Institute of Technology,
Harbin 150001, China

1 Introduction

Facing today's globalization environment and fast development of modern manufacturing industry, there is a demand to improve productivity continuously to remain competitiveness. Increases in welding productivity have a potential economic impact of several hundred million dollars in yearly worldwide savings [1]. Recently, gas metal arc welding (GMAW), the most widely used joining technology in industry, has been modified to improve welding productivity [2–4]. Through increasing the welding speed of GMAW, welding productivity can be raised. However, humping phenomena will occur when welding speed is beyond a certain limit (the so-called critical welding speed) [5, 6]. Humping bead, described as a series of periodic fluctuation of swellings on the weld bead (Fig. 1), is one of the dominating defects in high speed welding, which limits the wider application of high speed GMAW. Some modifications of GMAW process and/or development of novel processes have to be made to suppress or decrease the tendency for hump formation and achieve higher productivity welding.

Experiments have proved that laser–GMAW hybrid welding is able to operate at higher speed and to prevent the humping bead [7, 8]. But laser system requires huge equipment investment and high operation cost, which restricts its wide applications in industry. Because of their low cost and high suitability and adaptivity, GMAW processes should be modified to raise the welding speed further [9]. Tandem GMAW was invented to raise welding speed [10], but its higher welding speed is usually accomplished with higher level of welding current to produce enough amount of deposited metal, then it is easy to make the base metal be overheated. Previous investigations have illustrated that humping bead defect can be avoided if the heat energy is properly partitioned between the filler wire and the base metal during high speed welding [11], i.e., sufficient current flows through the wire to

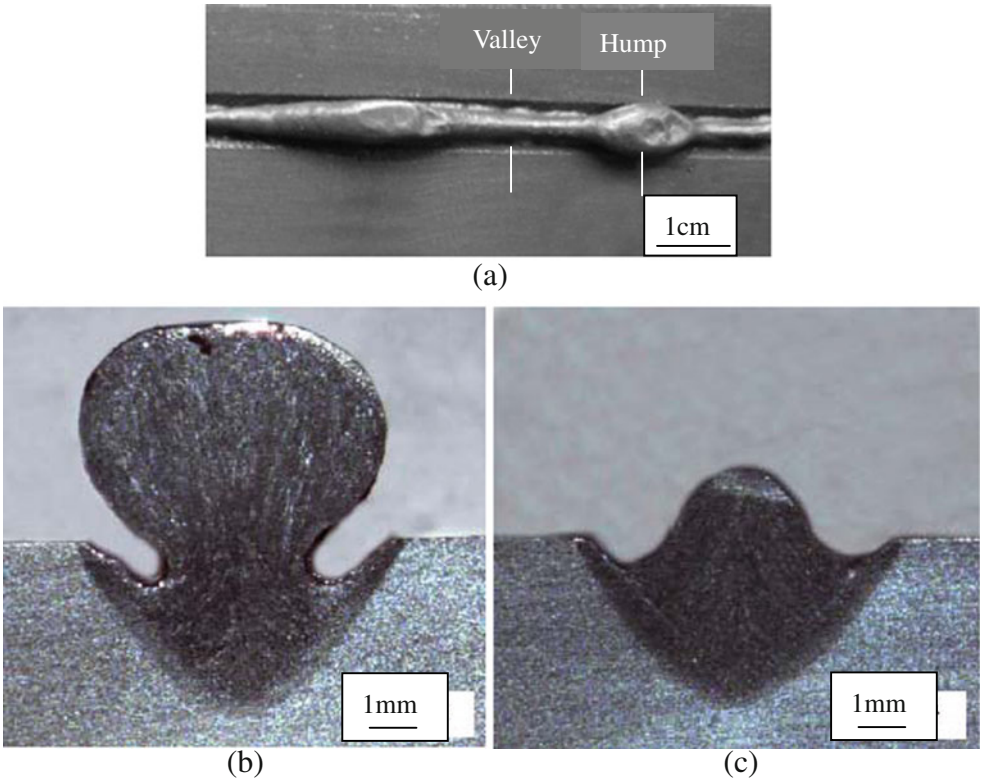

Fig. 1 Humping bead in GMAW (welding speed 1.5 m/min, welding current 350 A). **a** Weld bead apperance. **b** Transverse cross-section at hump. **c** Transverse cross-section at valley

ensure higher melting rate of wire while relative lower current flows through the workpiece to produce a weld pool with appropriate shape and size. For conventional GMAW processes, the welding current passing through the wire is equal to that acting on the base metal. Thus, it is difficult to further increase the welding speed while maintaining satisfactory amount of deposited metal in conventional GMAW. Zhang et al. developed a modified arc welding process, referred to as the double-electrode gas metal arc welding (DE-GMAW) [12–14], to decouple the base metal current from the wire current in GMAW so that high current can be used to melt the wire and to achieve high melting rate to fill the groove in a single pass while the heat input to the base metal is lowered. Therefore, DE-GMAW has the potential to solve the aforementioned contradiction (higher current on the wire and lower heat input on the base metal).

In this study, an experimental system was developed to implement DE-GMAW, humping bead defect was suppressed, and the welding speed limit was increased. A vision system was employed to observe the weld pool behaviors during GMAW and DE-GMAW, respectively. The reason why humping bead is prevented during high speed DE-GMAW is explained.

2 Experimental system and tests of DE-GMAW

As shown in Fig. 2, two power supplies (model YC-300TSPVTA for gas tungsten arc welding, GTAW, and model YD-350RF2HGE for GMAW) and two torches were linked together to constitute the experimental DE-GMAW system. The welding torches were kept stationary while the welding test-table carried the test plates to move. The GTAW torch was leading while the GMAW torch was trailing. The positive terminals of GTAW power supply and GMAW power supply were linked together. The total current (I) flows through the contact tip of GMAW torch to melt the wire. In the arc area, one part of current (I_{bp}) flows through the gas tungsten arc to the negative terminal of GTAW power supply, and the other part of current (I_{bm}) flows through the base metal to the negative terminal of

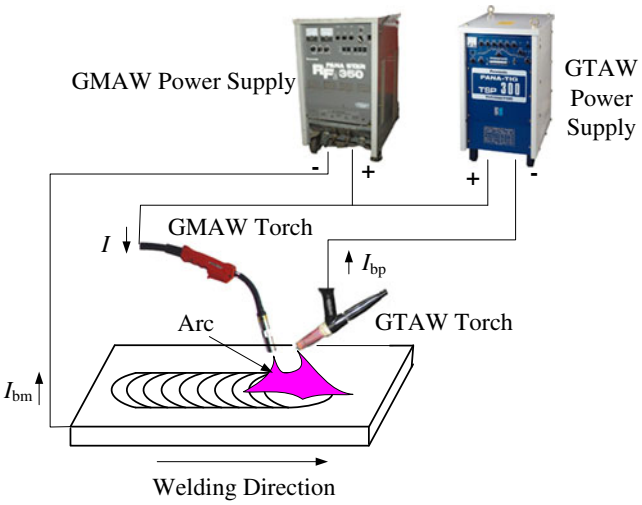

Fig. 2 Schematic diagram of DE-GMAW system

GMAW power supply. So the total current flowing through the wire (I) is divided into two parts, i.e., the bypass current (I_{bp}) and the base metal current I_{bm}. Then, it can increase the amount of deposited metal under relatively lower heat input to the base metal. The heat energy can be adjusted so that it is properly partitioned between the wire and the base metal.

As demonstrated in Fig. 3, there are six geometric parameters determining the relative position of the two torches, i.e., the contact tube to workpiece distance (d_1), the tungsten tip to workpiece distance (d_2), the wire–tungsten tip distance (d_3), and three angles (θ_1, θ_2, and θ_3). Their settings are very important for implementing DE-GMAW. The initial settings are as follows: d_1=20 mm, d_2=12 mm, d_3=4~7 mm (if d_3> 7 mm, it is difficult to ignite the gas tungsten arc; if d_3< 4 mm, it will promote the burning loss of tungsten electrode), θ_1=65°, θ_2=85°, and θ_3=30°.

A charge-coupled device (CCD) camera was used to observe the arc behavior during DE-GMAW process. To this end, the camera aims at the arc region from side view. The camera axis is perpendicular to the welding direction and is located above the workpiece surface. To start the DE-GMAW process, the GMAW power supply is turned on firstly, and gas metal arc (main arc) forms between the wire and the base metal (Fig. 4a). Then, the GTAW power supply is switched on, and gas tungsten arc (bypass arc) forms between the tungsten electrode and the gas metal arc (Fig. 4b). At the beginning, the gas tungsten arc is repelled by the gas metal arc (Fig. 4b). But as time goes on, the gas tungsten arc gradually overcomes this repelling action (Fig. 4c), and then takes an approximate direction along the tungsten axis (Fig. 4d). The arc configurations in Fig. 4 were taken when the distance d_2=12 mm. The experiments show that the weld bead appearance was poor when the distance from the tungsten electrode tip to the base metal takes a bigger value (d_2=12 mm). When d_2 was changed to 6 mm, the arc configuration is shown in Fig. 5, and the weld bead formation became better. At the upper part of gas tungsten arc, the magnetic field produced from the bypass arc has the same direction as that from the main arc, so that there is repelling action between two arcs at upper position.

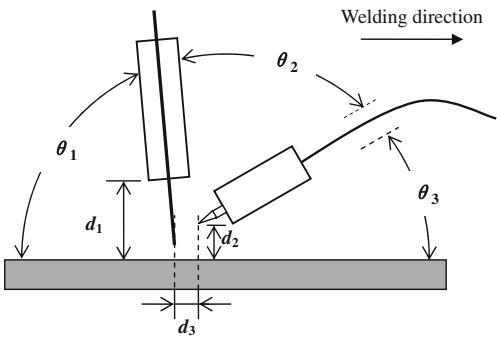

Fig. 3 The relative position of two torches

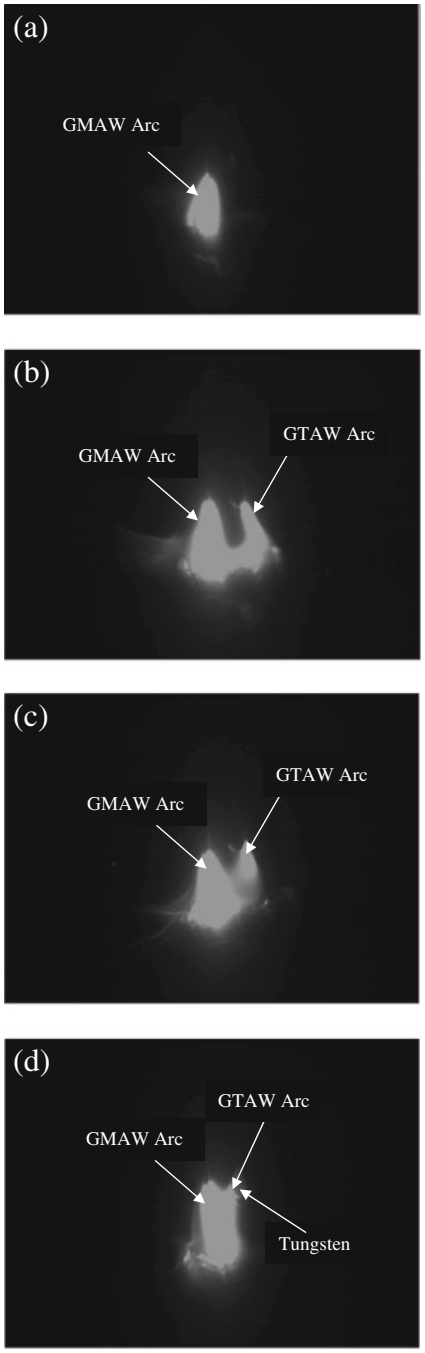

Fig. 4 The arc configurations in DE-GMAW (d_2=12 mm). **a** 0.45 s. **b** 0.68 s. **c** 0.90 s. **d** 1.24 s

At the lower part of gas tungsten arc, the bypass arc and main arc have opposite magnetic field directions, so that two arcs are attractive at lower position. If the value of d_2 is reduced, the contact point between the bypass arc (gas tungsten arc) and the main arc (gas metal arc) is lowered, so the applied force moment of the bypass arc to the main arc becomes less. Since the effect of the bypass arc on the main arc is lowered, its effect on the weld pool behaviors is lowered too. Thus, satisfactory weld bead formation is obtained.

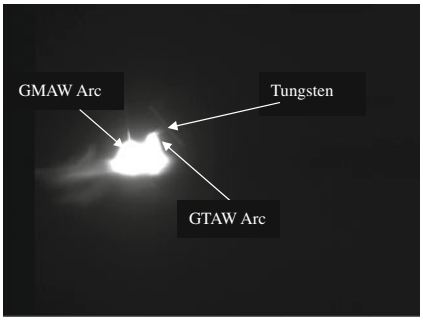

Fig. 5 The arc configurations in DE-GMAW (d_2=6 mm)

According to the standard of satisfactory weld bead formation, the ranges of d_2 and d_3 were determined as follows through DE-GMAW experiments: d_2=6~10 mm and d_3=4~7 mm. In this study, the parameters took the following values: d_2=7 mm, d_3=5 mm, d_1=20 mm, θ_1=65°, θ_2=85°, and θ_3=30°.

In the DE-GMAW tests, the wire diameter was 1.2 mm. The shielding gas of GMAW torch was Ar + 8%CO_2 with a flow rate of 10.8 L/min and the shielding gas of GTAW torch was pure Ar with a flow rate of 7 L/min. The base metals were Q235 low carbon steel plates of 6-mm thickness. Bead-on-plate welding was conducted with different welding speeds (ν_w). Because GTAW power supply has a characteristic of constant current and GMAW power supply has a characteristic of constant voltage, the bypass current I_{bp} took a value of 130 A while the main arc voltage took a value of 32 V.

In the welding process of DE-GMAW, different values of I_{bm} and I can be obtained by changing the welding current of GMAW power supply. During the welding process, the values of I, I_{bp}, and I_{bm} were measured by a computer through Hall element sensing unit under certain welding conditions, and the relationship about them was obtained. The effect of different settings (I, I_{bp}, and I_{bm}) on the weld bead formation and the welding speed limit were investigated.

Figure 6 shows the morphology of weld bead in DE-GMAW with bypass arc current of 130 A. No humping beads were formed at welding speed over 1.55 m/min. Thus, DE-GMAW can be operated in high speed welding up to 1.70 m/min.

3 Weld pool features without humping bead formation

Welding tests have shown that DE-GMAW is able to be operated at high speed without formation of humping bead (Fig. 6). To reveal the reason why DE-GMAW can suppress humping bead, a sensing system was developed to observe the weld pool behaviors during DE-GMAW process. The vision system includes the CCD camera (Model AM 1101),

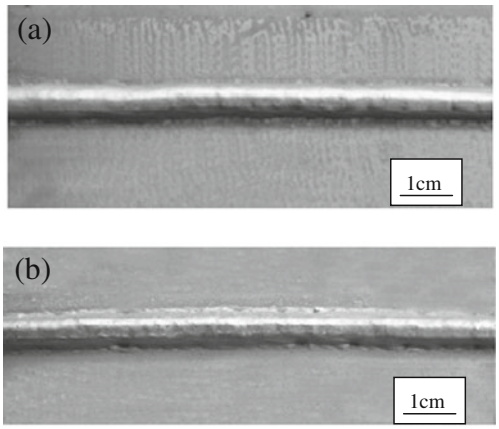

Fig. 6 The morphology of DE-GMAW welds (I_{bp}=130 A). **a** ν_w=1.55 m/min, I=306 A. **b** ν_w=1.70 m/min, I=326 A

narrow band-pass filter, image-grabber, and computer. The narrow band-pass filter with central wavelength of 610 nm and band width of 20 nm as well as a neutral density filter with transparency 10% was equipped to the CCD camera to eliminate the disturbance from the very intense arc light. The distance between the wire and the CCD lens is 47 cm.

The weld pool surface is of a complex curved profile. To obtain more information on the weld pool behaviors, an imaging way from the side view was proposed and implemented. As shown in Fig. 7, the camera axis is perpendicular

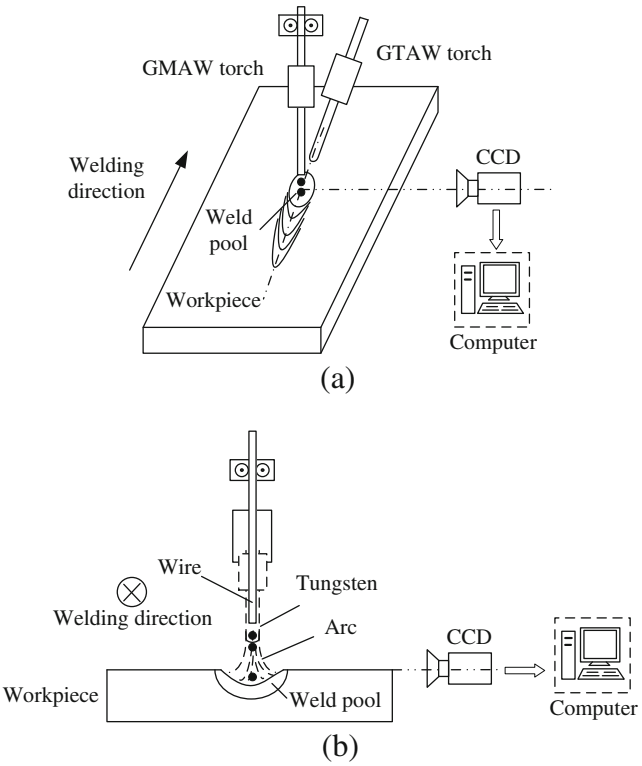

Fig. 7 Schematic of the vision system in DE-GMAW. **a** Schematic of three-dimensional set-up. **b** Planar graph of experimental set-up

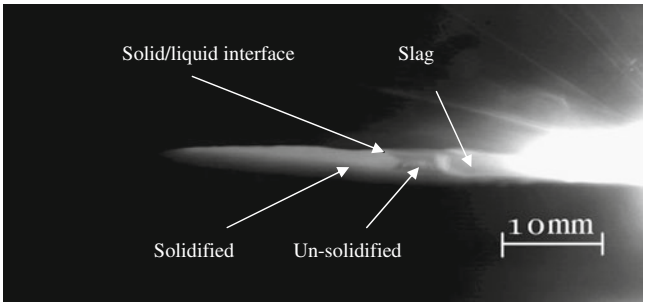

Fig. 8 Side view image of weld pool in DE-GMAW

to the welding direction, and is located on the workpiece surface with a wire–CCD axis angle of 90°. In this way, complete side view of weld pool can be imaged.

Figure 8 is one frame of the captured image of weld pool from side view during DE-GMAW. The right-hand side at the image is the pool front with some arc light. The left-hand side

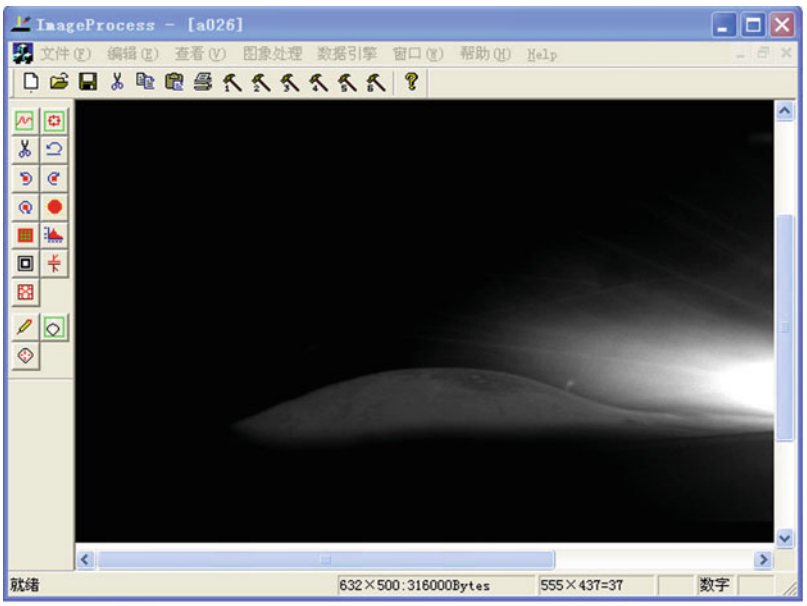

(a)

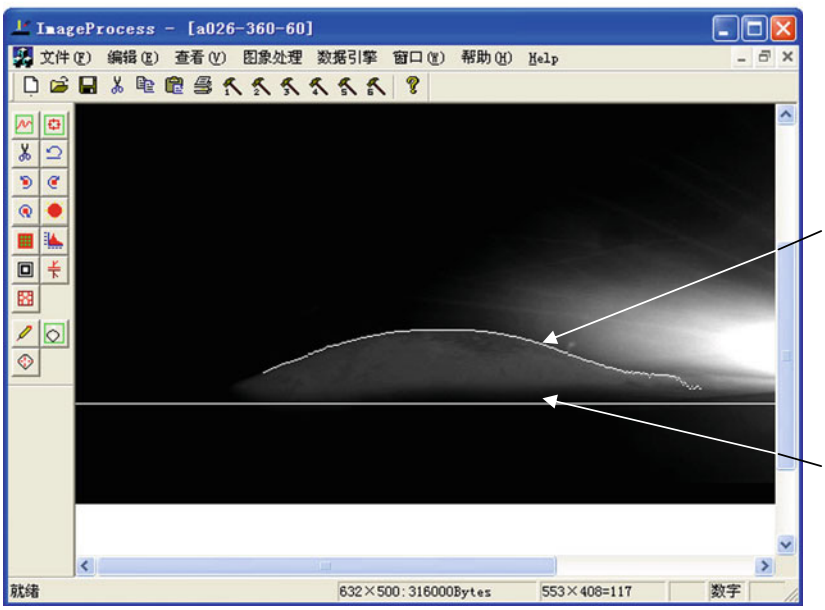

(b)

Fig. 9 The imaging process result. **a** Before processing. **b** After processing

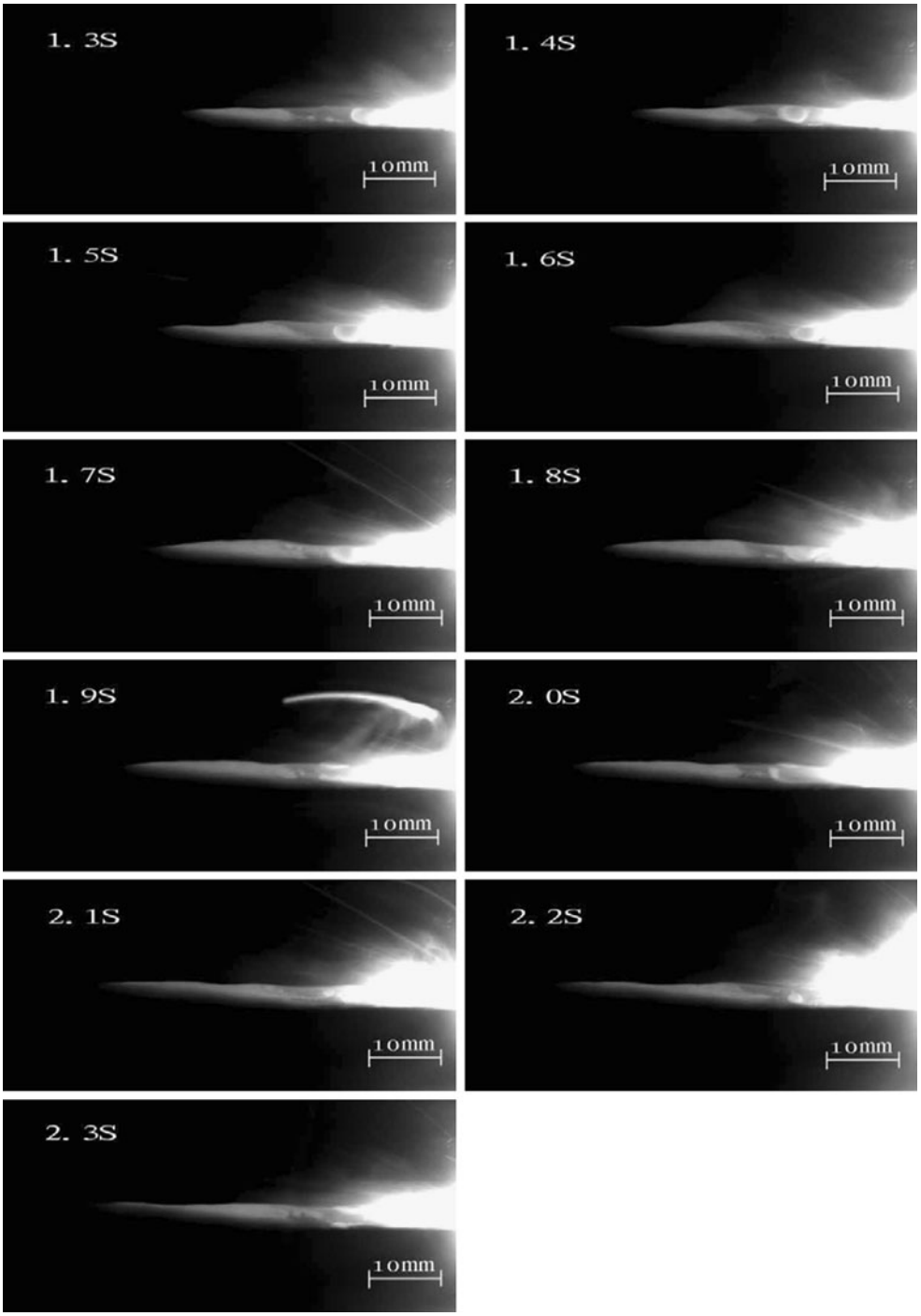

Fig. 10 Sequential side view images of weld pool during DE-GMAW. (ν_w=1.30 m/min I=316 A,U=32 V)

is the pool tail and the solidified weld region. The solid–liquid interface is clear. Since the camera axis is perpendicular to the welding direction, and is located on the workpiece surface as shown in Fig. 7, the bulk of molten metal at the rear of the weld pool can be observed from side view, and the height of weld pool tail can be obtained after image processing.

Figure 9a is one image of weld pool at rear part displayed in the window of image processing software which was self-developed. When the image of the weld pool captured by the CCD camera is digitized through frame-grabber, it is stored in computer as a matrix in which one element represents a dot of image. A brighter dot in the image corresponds to a higher value (gray value) of the element in the matrix. For the image captured as shown in Fig. 9a, the coordinates of a point in the image are expressed by (i, j), where i is the row number while j is the column number in the gray matrix. To extract the weld pool boundaries, the special image processing software has been developed, which includes the following three steps: (1) noise elimination; (2) enhancement; and (3) searching for edges [15]. Figure 9b is the weld pool image with marked

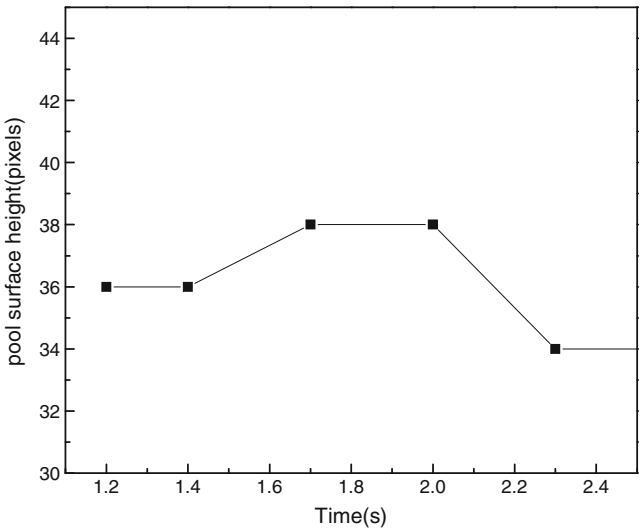

Fig. 11 The height of weld pool tail verse time during DE-GMAW (ν_w=1.30 m/min, without humping bead)

boundary after image processing. After extracting the edge points of the weld pool images, the coordinates of these edge points (i, j) are obtained and stored in an array. Because the actual size of the weld pool is different from the size of the digital image, a calibration must be carried out. After calibration, the real dimension of weld pool boundary can be determined. The self-developed image processing and calibration algorithm have been introduced in detail in [15] and is not repeated again here. Therefore, based on the processed images in Fig. 9b, the surface height of weld pool can be determined.

Figure 10 demonstrates the side view images of weld pool during a period of 1 s (from 1.3 to 2.3 s). The corresponding DE-GMAW test conditions were as follows: welding current I=316 A, I_{bp}=130 A, main arc voltage U=32 V, and welding speed ν_w=1.30 m/min. Other parameters are as aforementioned. Checking out the images at the rear part of the weld pool in Fig. 10, it is found that the height of both solidified and molten region at the pool tail is almost flat when no humping bead is formed during DE-GMAW. After image processing, the pool tail height can be characterized as the amount of pixels. Figure 11 shows the variation of pool tail height with time. During DE-GMAW, the pool tail height is around 36 pixels. This means that no molten metal accumulation takes place at the pool tail

Fig. 12 The weld bead morphology in GMAW (ν_w=1.30 m/min, I=321 A, U=30 V)

during DE-GMAW process, so that no humping bead forms there.

To compare the observed weld pool behaviors in DE-GMAW to that in GMAW, conventional GMAW tests were made. For conventional GMAW, when the welding speed is 1.30 m/min under the condition of welding current 321 A and arc voltage 30 V, humping bead forms, as shown in Fig. 12. The vision system was also used to capture the side view images of weld pool during GMAW process. Figure 13 shows the sequential side view images of weld pool when humping bead forms in GMAW. At the initial stage, molten metal is pushed from the pool front to the pool tail, and there is accumulation of liquid metal there. The backward flow of molten metal inside the weld pool is responsible for the initial formation and the growth of a hump which itself is promoted by the high surface tension of molten metal. The strong momentum of the backward flow of molten metal inside the wall jet prevents backfilling of the front portion of the weld pool, which leads to the elongation and ultimately the solidification of the wall jet to form a valley in a humped weld bead [5, 6, 16–18]. At the moment of 2.6 s, a hump has formed. It should be noted that the peak height of humped pool surface locates at the middle part, as shown in the images at 2.4 s–2.6 s in Fig. 13. The humping height of weld pool surface increases with time during the forming process of a hump, as demonstrated in Fig. 14. The humping height of pool surface at the middle part changes from 45 to 60 pixels. It is quite different from the case in DE-GMAW (Fig. 11).

Investigators have proposed a few models to explain the occurrence of humping bead in high speed welding. Mendez and Eagar proposed a simple model to determine the force balance at the transition line which delimits the sharp transition between the gouged region at the front part and the trailing region inside weld pool and predict the onset of humping in GTAW [1]. Kumar and DebRoy developed a phenomenological model based on the stability of waves on the weld pool surface due to relative motion between the plasma and the liquid weld metal to examine the conditions for the formation of humping defect in GTAW [19]. For GMAW, Bradstreet [20] and Gratzke et al. [21] used capillary instability model to explain the humping phenomenon, which simplified the molten pool as a liquid cylinder. Nguyen et al. found that the strong momentum of the backward flow of molten metal in the weld pool that typically occurred during high speed GMAW was the major factor responsible for the initiation of humping [5, 6]. Figures 10 and 11 demonstrate that the pool tail height is almost kept flat during DE-GMAW and no swelling of molten metal occurs there. This shows that the momentum of the backward flow of molten metal in the weld pool is lowered during DE-GMAW process. For DE-GMAW process, the main arc and the bypass arc combine together to form a little

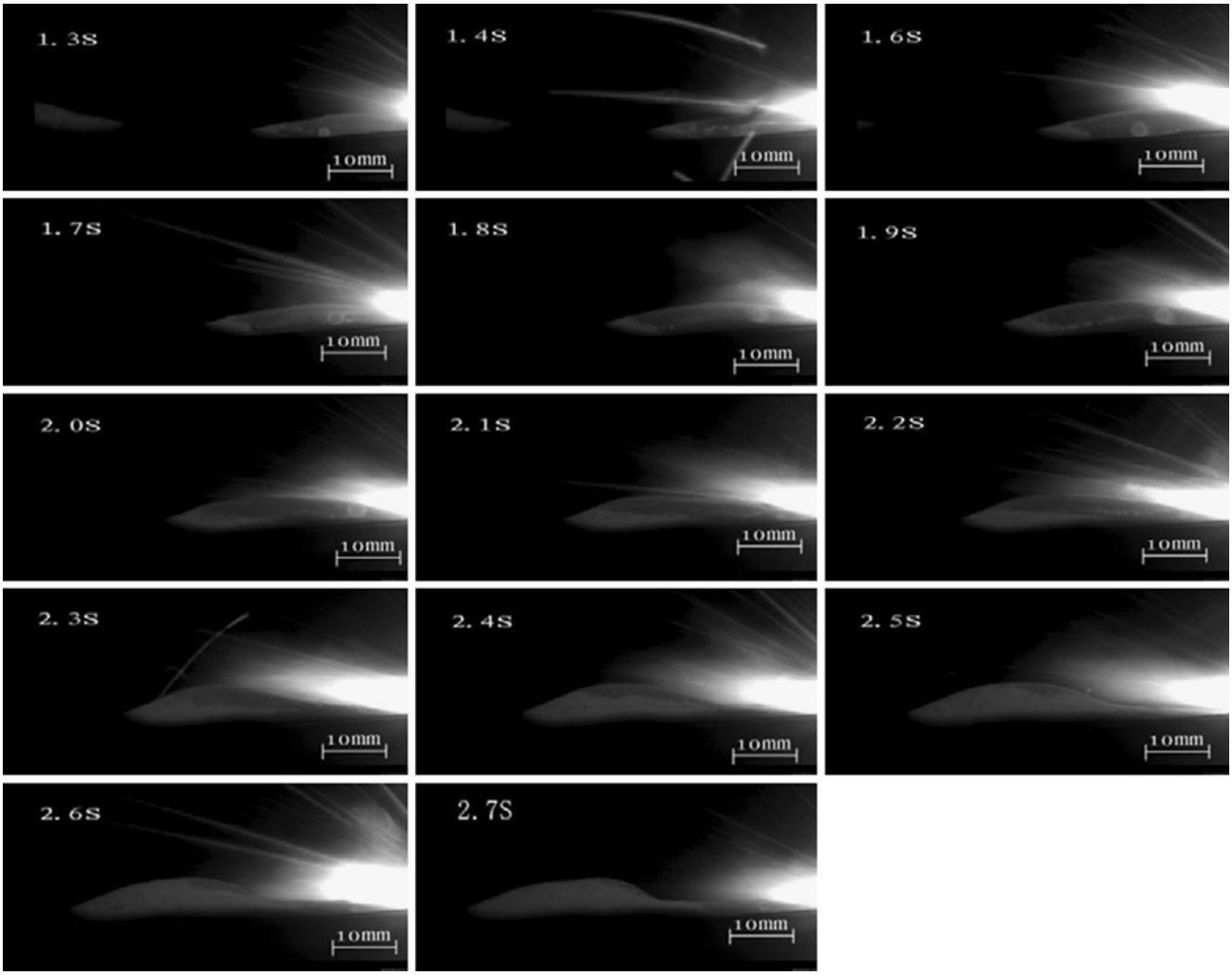

Fig. 13 Sequential side view images of weld pool when humping bead forms in GMAW (ν_w=1.30 m/min, I=321 A, U=30 V)

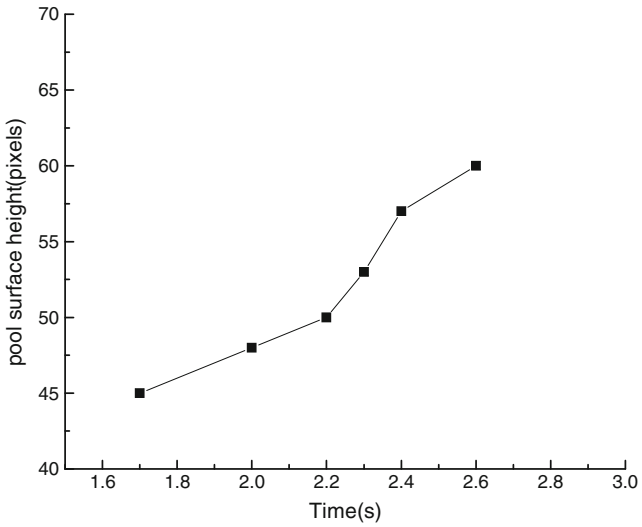

Fig. 14 Variation of humping height of weld pool surface when humping bead forms in GMAW (ν_w=1.30 m/min, I=321 A, U=30 V)

bit larger arc configuration and the contact area between the arc and the workpiece gets relatively bigger. The larger arc–workpiece contact area makes the arc pressure be distributed in a larger region so that the arc force is not overcentralized. A more uniform distribution of arc force produces a less severe depression of weld pool surface underneath the arc. This causes a thicker molten layer at the pool front which can absorb some momentum of transferring droplets. The lowering of both arc force concentration and droplet momentum decreases the momentum of the backward flow of molten metal in the weld pool so that DE-GMAW process can suppress the formation of humping bead.

4 Conclusions

1. An experimental system was developed to implement DE-GMAW which appropriately divides the total current flowing through the wire into the bypass current

and the base metal current. The heat energy can be properly partitioned between the wire and the base metal, and high speed welding can be realized.

2. The arc images were captured during DE-GMAW process. Based on the observed arc configurations, the geometric parameters between two torches were optimized. Thus, the main arc and bypass arc integrated well and satisfactory weld bead formation is obtained.
3. A sensing system was developed to observe the weld pool behaviors from side view during DE-GMAW process. It is found that the height of both solidified and molten region at the pool tail was almost flat when no humping bead was formed during DE-GMAW. The DE-GMAW system is able to lower both arc force concentration and droplet impact so that the momentum of the backward flow of molten metal in the weld pool is weakened and no molten metal accumulation takes place at the pool tail during DE-GMAW process. This is the reason why DE-GMAW can prevent from humping bead.

Acknowledgments The authors are grateful to the financial support for this project from the State Key Lab of Advanced Welding & Joining, Harbin Institute of Technology under grant no. 09005.

References

1. Mendez PF, Eagar TW (2003) Penetration and defect formation in high-current arc welding. Weld J 82(10):296s–306s
2. Pires I, Quintino L, Amaral V, Rosado T (2010) Reduction of fume and gas emissions using innovative gas metal arc welding. Int J Adv Manuf Technol 50(5–8):557–567
3. Ding M, Tang XH, Lu FG, Yao S (2011) Welding of quenched and tempered steels with high-spin arc narrow gap MAG system. Int J Adv Manuf Technol 55(5–8):527–533
4. Shao Y, Wang ZZ, Zhang YM (2011) Monioring of liquid droplets in laser-enhanced GMAW. Int J Adv Manuf Technol 57(1–4):203–214
5. Nguyen TC, Weckman DC, Johnson DA, Keer HW (2006) High speed fusion weld bead defects. Sci Technol Weld Join 11(6):618–633
6. Nguyen TC, Weckman DC, Johnson DA, Keer HW (2005) The humping phenomenon during high speed gas metal arc welding. Sci Technol Weld Join 10(4):447–459
7. Choi HW, Farson DF, Cho MH (2006) Using a hybrid laser plus GMAW process for controlling the bead humping defect. Weld J 85(8):174s–179s
8. Choi HW, Farson DF (2007) Simulation study of a hybrid process for the prevention of weld bead hump formation. Weld J 86 (9):253s–262s
9. Zhang YM, Zhang SB, Jiang M (2002) Keyhole double-sided arc welding process. Weld J 81(11):249s–255s
10. Lu ZY, Huang PF, Jiang GJ (2006) Study status of techniques and mechanism of high-speed MIG/MAG welding. Weld Joining 3:16–20
11. Wu CS, Zhang MX, Li KH, Zhang YM (2007) Study on the process mechanism of high speed DE-GMAW. Acta Metallurgica Sinica 43(6):663–667
12. Zhang YM, Jiang M (2004) Double electrodes improve GMAW heat input control. Weld J 83(11):39–41
13. Li KH, Zhang YM (2007) Metal transfer in double-electrode gas metal arc welding. J Manuf Sci Eng-Transact ASME 129(6):991–999
14. Li KH, Chen JS, Zhang YM (2007) Double-electrode GMAW process and control. Weld J 86(8):231s–237s
15. Wu CS, Gao JQ, Wang DM (2011) Observation of weld pool profiles in short-circuiting gas metal arc welding. Proc Instn Mech Engrs, Part B: J Eng Manuf 225(10):1873–1887
16. Hu ZK, Wu CS (2008) Experimental investigation of forming process of humping bead in high speed MAG arc welding. Acta Metallurgica Sinica 44(12):1445–1449
17. Wu CS, Zhong LM, Gao JQ (2009) Visualization of hump formation in high speed gas metal arc welding. Meas Sci Technol 20 (11):115702. (8pp). doi:10.1088/0957-0233/20/11/115702
18. Chen J, Wu CS (2010) Numerical analysis of forming mechanism of hump bead in high speed GMAW. Weld World 54(9/10):R286–R291
19. Kumar A, DebRoy T (2006) Toward a unified model to prevent humping defects in gas tungsten arc welding. Weld J 85(12):292s–304s
20. Bradstreet BJ (1968) Effect of surface tension and metal flow on weld bead formation. Weld J 47(7):314s–322s
21. Gratzke U, Kapadia PD, Dowden J, Kroos J, Simon G (1992) Theoretical approach to the humping phenomenon in welding processes. J Phys D: Appl Phys 25(11):1640–1647